



Research article

Honeybee pollen assisted biosynthesis of nanogold and its application as catalyst in reduction of 4-nitrophenol

Brajesh Kumar^{a,b,*}, Kumari Smita^b, Yolanda Angulo^b, Alexis Debut^b, Luis Cumbal^b^a Department of Chemistry, TATA College, Kolhan University, Chaibasa, 833202, Jharkhand, India^b Centro de Nanociencia y Nanotecnología (CENCINAT), Universidad de Las Fuerzas Armadas ESPE, Av. Gral. Rumĩnahui S/n, Sangolquí, P.O. BOX 171-5-231B, Ecuador

ARTICLE INFO

Keywords:

Honeybee pollen
Gold nanoparticles
Catalysis
UV-Vis spectroscopy
TEM
Ecofriendly

ABSTRACT

Nowadays, the exploration of natural materials for the production of nanoparticles is of special interest due to its ecofriendly nature. In this paper, we presented the biosynthesis of gold nanoparticles (AuNPs) in a green route by using water extract of pollen from Andean honeybees. Furthermore, AuNPs have been characterized by various techniques and tested for the catalytic reduction of 4-nitrophenol (4-NP). The biosynthesized AuNPs were analyzed using UV-vis spectroscopy, Transmission electron microscopy (TEM), Dynamic light scattering (DLS), Fourier transform infrared spectroscopy (FTIR), and X-ray diffraction (XRD) spectroscopy to confirm their optical properties, stability, surface morphology, and purity. The synthesized AuNPs proved to be well dispersed, spherical, and triangular in shape, with particle sizes ranging from 7 to 42 nm having λ_{\max} at 530 nm. Moreover, FTIR suggests the capping of AuNPs with pollen constituents and XRD confirms the crystalline structure of AuNPs. Additionally, prepared AuNPs were demonstrated to be effective in reducing organic pollutant 4-NP to 4-aminophenol ($k = 59.17898 \times 10^{-3} \text{ min}^{-1}$, $R^2 = 0.994$). All of these studies have emphasized that AuNPs production can be scale up by using naturally available pollen grains and open up a new perspective for beekeepers.

1. Introduction

Nanotechnology and Nanoscience deal with the manipulation of atoms and molecules, in nanoscale materials (1–100 nm) and exhibit extraordinary physicochemical properties like area-volume ratio, physical, chemical, optical and electronic properties [1]. Metallic nanoparticles (MNPs) are generally synthesized with hazardous chemicals, high temperature, high pressure, energy, and toxic effects on human and aquatic life [2]. However, nanoparticles from precious metals, like gold, silver, platinum, and palladium are extensively used in products that come into direct contact with the human body, such as shampoos, soaps, detergents, footwear, cosmetics, and toothpastes, as well as biomedical and pharmaceutical applications, with gold having a long history of usage [3]. In addition, gold nanoparticles (AuNPs) require the desired reducers and stabilizers to maintain their morphology.

To date, several ecofriendly and green chemistry approaches have been identified for AuNPs synthesis without the use of hazardous chemicals and high operational costs, in order to overcome the challenge of environmental pollution [4]. Extracts from natural sources like

microbes, algae, natural polymers, and plants contain many bioactive molecules that act as reducing and capping agents, and cause synthesis of MNPs [5]. Recently, extracellular biosynthesis methods using different extracts of natural materials, including *Padina gymnospora* macroalga [3], *Plukenetia volubilis* leaf [6], vegetable waste [7], *Plumeria alba* flower [8], *Prunus serotina* fruit [9], *Nephelium lappaceum* fruit peel [10], *Dracopcephalum kotschyi* leaf [11], Cyanobacteria algae [12], *Calothrix* algae [13], *Angelica gigas* stem [14], *Mangifera indica* flower [15], *Datura stramonium* seed [16], *Blighia sapida* husk [17], *Persea americana* fruit peel [18], *Enterococcus* species [19], *Trichoderma longibrachiatum* and *Aspergillus niger* xylanases enzyme [20], honey [21], pine cone pollen [22], date palm pollen [23], have already been reported to synthesize AuNPs. In the present study, we investigated the biogenic approach to the synthesis and characterization of AuNPs using bee pollen, and its catalytic activity to remove 4-nitrophenol (4-NP), a hazardous organic pollutant (Figure 1).

Bee pollen, a natural material commonly known for its elegant colour and used in the human diet since ancient times. It is rich in flavonoids, amino acids, fatty acids, etc [24]. They have numerous medicinal properties including antimicrobials, antidiabetics, antispasmodics,

* Corresponding author.

E-mail addresses: krmbraj@gmail.com, krmbrajnano@gmail.com (B. Kumar).

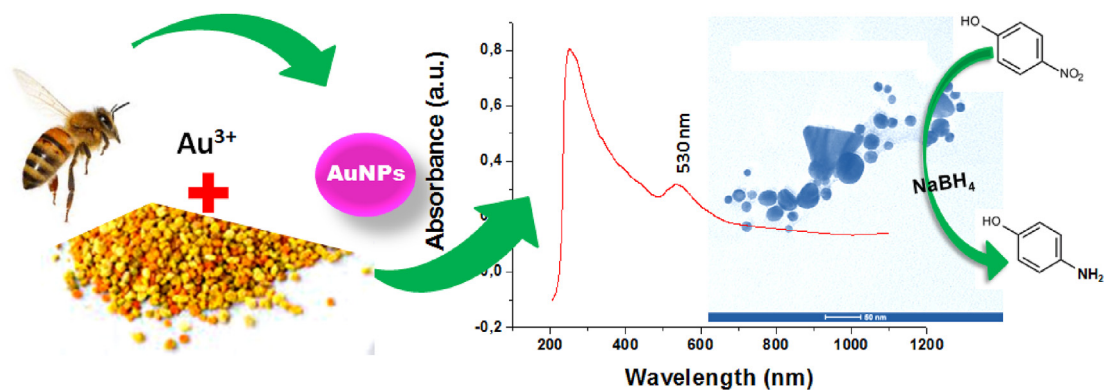


Figure 1. Diagrammatic representation of bee pollen assisted biosynthesis of AuNPs, characterization and its catalytic activity.

anticancers, and antioxidants [25]. A review by Lateef and co-workers has already documented the importance of arthropods and their metabolites in the biosynthesis of various MNPs [26].

Nitrophenols are the most common organic contaminants in aquatic environments, including industrial and agricultural wastes. Among all nitrophenolic compounds, 4-NP is an important raw material used in various chemical industries (dye, electronics, textiles, food, medicine, agrochemical) and is stable in aqueous media for an extended period of time. Its excessive use poses several environmental and health hazards including shortness of breath, nausea, cyanosis, methemoglobinemia, fervecence, liver and kidney damage, dizziness, headaches, etc., to humans [27, 28]. Therefore, removal of 4-NP from the environment is of great interest and a challenging task for the scientist. Our study was focused on the physicochemical analysis and catalytic activity of bio-synthesized AuNPs.

2. Materials and methods

2.1. Materials

Honeybee pollen was purchased from local beekeepers (November 2013) near ESPE, Sangolqui, Ecuador ($0^{\circ}21'30.9''$ S $78^{\circ}25'38.9''$ W). Beekeepers are enrolled in the National Beekeeping Health Program and originate from the province of Pichincha, situated in the inter-Andean region of Ecuador. Gold chloride (AuCl_3 , >99.8 %) and 4-Nitrophenol

(>99.5%, 4-NP) were acquired from Spectrum, USA. Sodium borohydride (NaBH_4 , >99.5%) was procured from Sigma-Aldrich, USA, and Milli-Q water was used for all aqueous solutions. All glassware has been cleaned with aqua regia and carefully flushed with Milli-Q water before use.

2.2. Preparation of pollen extract

For the preparation of the pollen extract, 250 mg of dark yellow honeybee pollen was homogenized with a pestle and porcelain mortar, and added to a 50 mL flask containing 10 mL of Milli-Q water. It was then stirred for 15 min at ambient temperature and centrifuged at 6000 rpm for 5 min to remove unwanted aggregates from the pollen extract solution. A clear supernatant from pollen extract was used for AuNPs synthesis.

2.3. Biogenic synthesis of AuNPs

For the biogenic synthesis of AuNPs, 500 μL of the pollen extract was blended with 4.5 mL of 0.5 mM AuCl_3 solution and incubated at $25 \pm 2^{\circ}\text{C}$ for 24 h. The visual colour shift from light yellow to light magenta was observed in the reaction mixture, confirming the synthesis of AuNPs. The reaction mixture was subsequently centrifuged at 10,000 rpm for 30 min (3×10 min) and maintained at 4°C for further instrumental characterization.

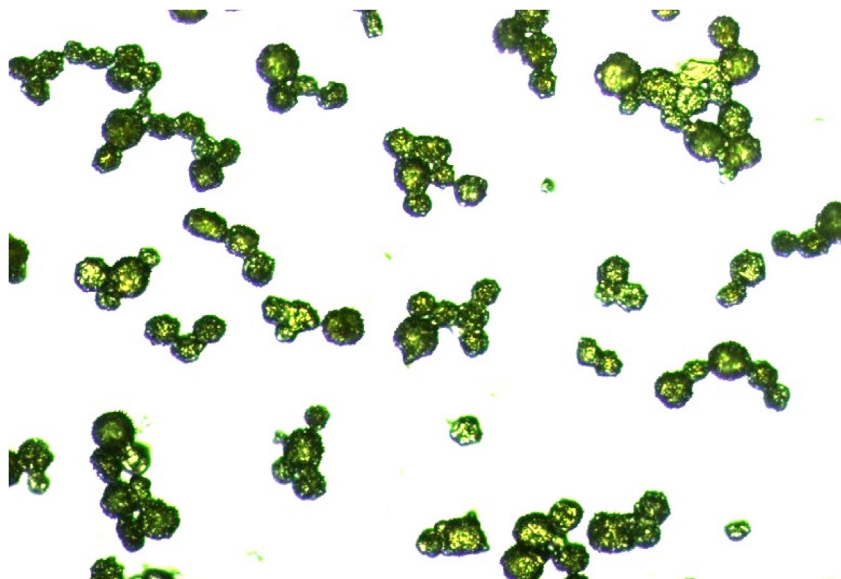


Figure 2. Digital microscopic image of honeybee pollen.

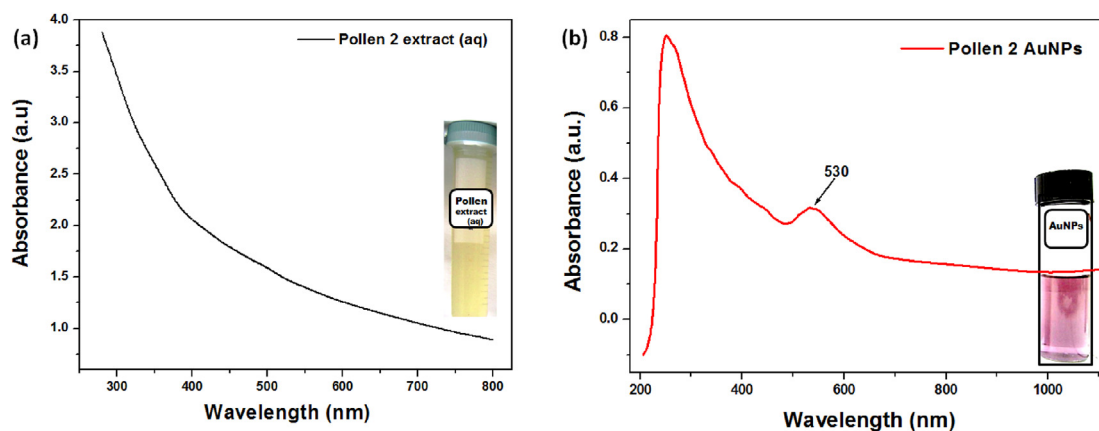


Figure 3. UV-vis spectrum of (a) pollen extract (aq) and (b) synthesized AuNPs [Inset: (a) aqueous extract of pollen and (b) synthesized AuNPs].

2.4. Spectroscopic and microscopic characterization of AuNPs

A digital microscopic image of bee pollen was obtained with the help of the Trinocular Stereomicroscope (SMZ745T, Nikon, Japan). The biosynthesis of AuNPs and its catalytic activity was determined by visual inspection and checking the absorption spectra using UV-visible spectrophotometer (Thermo Spectronic, GENESYS™ 8, England) and (SPECORD® S600 from Analytik Jena, Germany). The shape/size and selective area electron diffraction (SAED) pattern of AuNPs are studied by placing a drop of AuNPs on a carbon coated copper disc and visualizing it using high resolution transmission electron microscopy, HR-TEM (FEL, TECNAI, G2 spirit twin, Holland) having 80 kV accelerating voltage. The average particle diameter and Dynamic Light Scattering (DLS) of the AuNPs was determined using the HORIBA, DLS version LB-550 program (Japan). The Fourier transform infrared spectroscopy (FTIR) measurements of pollen and AuNPs in the attenuated total reflectance (ATR) mode were recorded using Frontier FT-IR spectrophotometer (Perkin Elmer, USA) to identify bee pollen constituents responsible for synthesis and capping of AuNPs. The UV-vis and FTIR graphics have been drawn on the OriginPro 8 program. The geometry of AuNPs was examined using X-ray diffraction (XRD) analyses (PANalytical, Malvern copper $\lambda = 1.54059$ Å and EMPYREAN diffractometer, UK) at 45 kV and 40 mA.

2.5. Catalytic activity of AuNPs

The catalytic activity of biosynthesized AuNPs was determined by carrying out the reduction of 4-NP to 4-AP (4-amino phenol) in the presence of NaBH_4 at 23–25 °C. About 3.4 mL of Milli-Q water, 200 μL of 2 mM

4-NP solution, and 200 μL of AuNPs were mixed into quartz cuvette. To this reaction mixture, 200 μL of NaBH_4 (0.05 mM) solution was added. For the non-catalyzed reaction, AuNPs were replaced with an equal quantity of Milli-Q water. The variation of UV-vis absorption spectra were monitored for 30 min at $\lambda = 230$ –550 nm and the rate constant (k) for the reduction process was determined by decrease of λ_{max} at 400 nm. The respective first order “ k ” can be calculated according to following equation.

$$kt = \ln(A_0/A_t) = \ln(C_0/C_t) \quad (1)$$

where A_0 , A_t , C_0 , and C_t are the initial absorbance/concentration of 4-NP at time (t) = 0 and final absorbance/concentration after t minutes. The linear relationship between $\ln(A_0/A_t)$ and time suggests the 1st order kinetics [13, 28].

3. Results and discussion

3.1. Microscopic image analysis of pollen

Light microscopic data collected from honeybee pollen explain the structural form and size of the pollen (Figure 2). It is evident that the pollens are spherical, rough, containing many round-tipped spines with sizes ranging from 15 to 50 μm . Pollens of different sizes are grouped together.

3.2. Visual and UV-Visible spectroscopy studies

The biosynthesis of AuNPs was initially confirmed by a colour change, from pale yellow to light magenta colour (Figure 3, Inset),

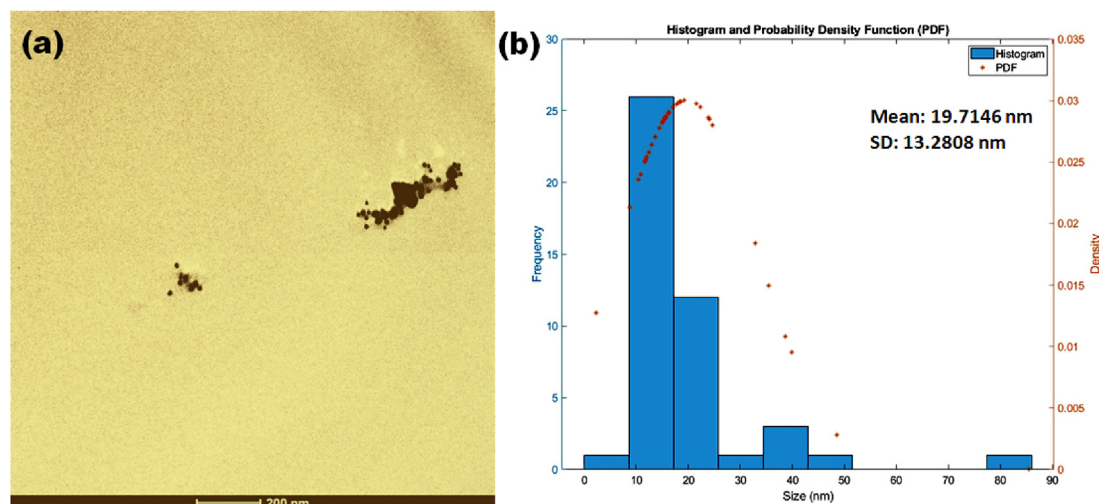


Figure 4. (a) TEM image and (b) size distribution graph of bee pollen synthesized AuNPs.

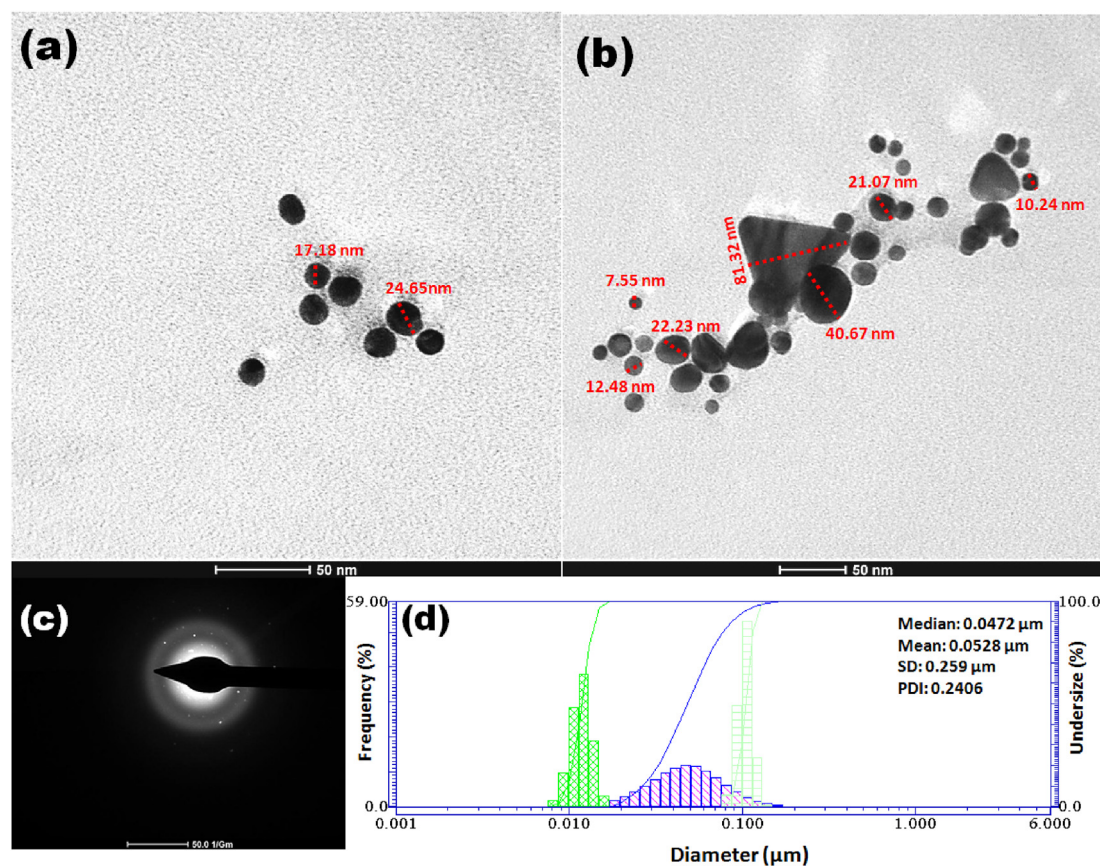


Figure 5. (a, b) HR-TEM images, (c) SAED pattern, and (d) DLS size distribution pattern of bee pollen synthesized AuNPs.

resulting in characteristic light absorption at a wavelength of 500–600 nm [9, 10]. The colour change is observed because of their optical properties, like excitation of surface plasmonic resonance vibrations (SPR) [15, 18, 20]. Figure 3 depicts the UV-vis spectrum of the pollen extract and as-synthesized AuNPs. The broad spectrum slope of 300–600 nm (Figure 3a) corresponds to the constituents of beepollen such as, flavonoids, amino acids, sugar, fatty acids, etc [29]. After synthesis, the UV-visible spectrum showed a new absorption peak at λ_{\max} 530 nm (Figure 3b) corresponding to the SPR of AuNPs, and confirm that spherical AuNPs are formed [30, 31]. Therefore, the light magenta colour in the reaction mixture is associated with the reduction of Au^{3+} to Au^0 ($\text{Au}^{3+} + 3\text{e}^- \rightarrow \text{Au}^0$) by the bee pollen constituents and formation of AuNPs. Similar outcomes were reported by Philip 2009 [21], Yu et al., 2016 [31], and Kumar et al., 2016 [30] using honey, *Citrus maxima*, and *Genipa americana* fruits.

3.3. TEM, SAED and DLS studies

In Figure 4, TEM analysis was performed to evaluate the morphology and distribution pattern of the AuNPs. The corresponding size distribution histogram of the AuNPs seen in the TEM image (Figure 4a) was analyzed manually with the ImageJ software. It demonstrated that the mean size of the structurally varied AuNPs was 19.72 ± 13.28 nm (Figure 4b).

To understand the clear morphology of AuNPs, HR-TEM was performed at a resolution of 50 nm and it reveals that the biosynthesized AuNPs were mainly spherical with sizes varying from 7 to 42 nm (Figure 5a, b). These findings are in agreement with the pattern of the SPR band recognized from the UV-visible spectrum with maximum absorption at 530 nm [6, 9]. All nanoparticles were widely dispersed, without aggregation suggesting the presence of hydrophobic coating around AuNPs. Few AuNPs are triangular and bigger than spherical

particles. The concentric ring of the SAED patterns (Figure 5c) indicated that these AuNPs were predominantly spherical (111) orientation, polycrystalline, and formed by the reduction of metallic ions [15, 18, 30]. The DLS analysis confirmed the size distribution and polydispersity index (PDI) of AuNPs in the aqueous medium (Figure 5d). DLS analysis revealed the average particle size for the AuNPs as 52.8 ± 25.9 nm with PDI of 0.2406. The size of the synthesized AuNPs was larger as presented by the DLS compared to TEM. The difference in the mean size as estimated by TEM and DLS occurs because in TEM, dry specimen is used for analysis while in DLS the aqueous dispersion of particles is measured [6]. This also may be due to the screening of smaller particles by a larger one or the presence of stabilizers/capping agents and hydration layer around the particles [9, 10, 28].

3.4. FTIR and XRD spectroscopy studies

The FTIR measurement was carried out to confirm the coating/capping of the AuNPs with the beepollen constituent. The presence of well-defined bands at 3254, 1658, 1453, 1224, 879, and 726 cm^{-1} (Figure 6a) confirm the presence of $-\text{OH}$, $-\text{NH}_2$, $-\text{CHO}$, $-\text{C}=\text{C}$, $\text{C}-\text{O}-\text{C}$, $\text{C}-\text{H}$ groups. The corresponding bands were attributed to the presence of chemical constituents (polyphenol, polysaccharide, fatty acid, and protein) in the pollen extract [32, 33]. A broadband near 2195 cm^{-1} may correspond to $\text{C}=\text{C}/\text{C}=\text{N}$ stretching band. For pollen coated AuNPs (Figure 6b), the characteristic wavenumber values are slightly shifted and the band intensity has changed compared to the pollen extract spectrum. The shifted bands observed at 3350, 2136, 1638, 1016, and 719 cm^{-1} may be suggested for the presence of the mentioned functional group on the AuNPs surface. In addition, the bands at 1453 and 1224 cm^{-1} (Figure 6a) disappear as a result of NPs formation. It is proposed that Au^{3+} ions can bind with $-\text{OH}$, $\text{C}=\text{O}$, or $\text{C}-\text{O}-\text{C}$ groups present in the pollen proteins or carbohydrates and form organometallic complexes,

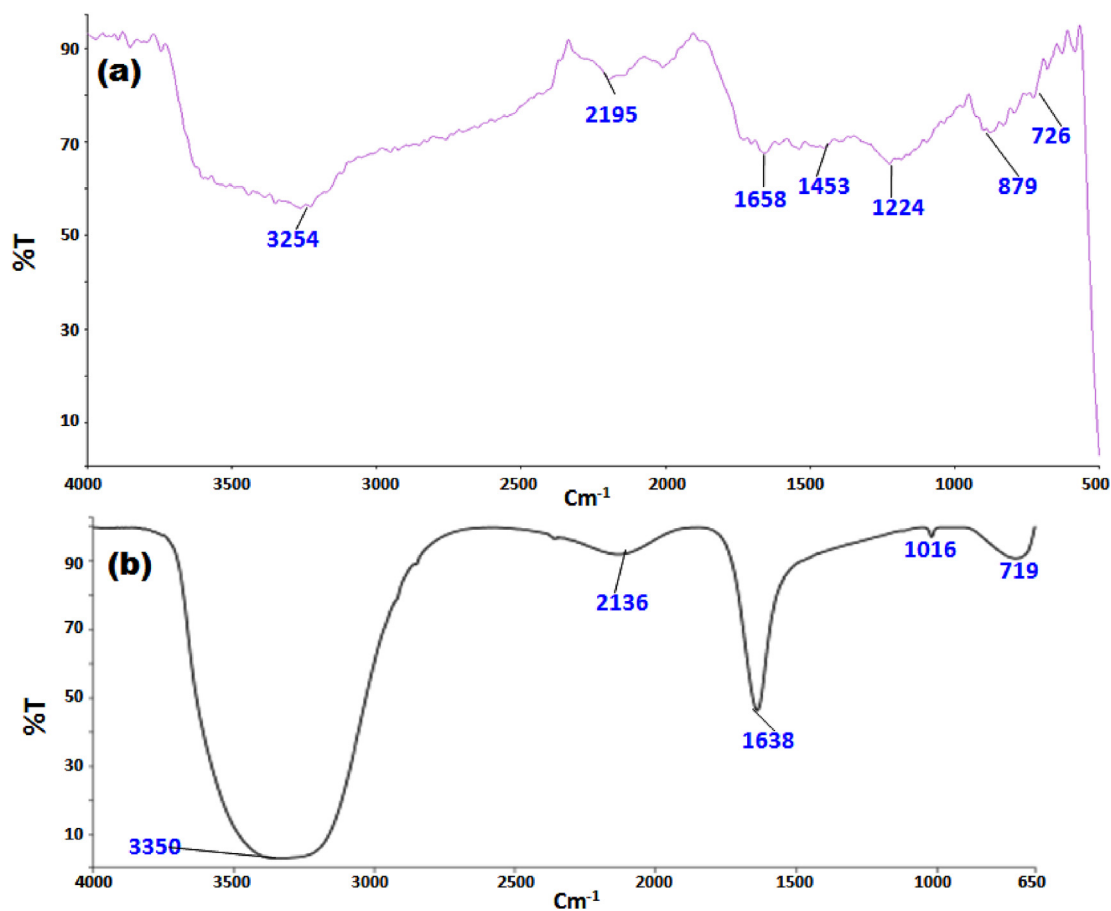


Figure 6. FTIR-ATR spectrum of (a) pollen extract and (b) synthesized AuNPs.

that subsequently oxidized to $-CHO/-COOH$ with a substantial reduction of Au^{3+} to Au^0 and the formation of AuNPs [31, 34].

Further, the structural composition and crystallinity of nanoparticles is determined by the XRD technique. XRD patterns for the pollen-coated AuNPs samples are shown in Figure 7. Clearly, four characteristic diffraction peaks can be observed at $2\theta = 38.14^\circ$, 44.41° , 64.75° and 77.78° which could be indexed to the (111), (200), (220), and (311) of Bragg reflection planes (ICSD No: 98-005-3763). Thus face-centered cubic (FCC) phase structure has been determined for

metallic gold/AuNPs. In addition, the extra-wide peak around 20° – 30° and some weak unidentified peaks (50° – 63°) observed in AuNPs, because of the presence of a organic layer/bioorganic phase on the particle surface. It can also be noticed that the peak corresponding to the (111) plane is stronger than the other planes, suggesting that (111) is the dominant orientation, as evidenced by the TEM-SAED image (Figure 5c). The XRD results are consistent with various reported values, confirming the cubic structure of phytosynthesized AuNPs [6, 21, 30, 31].

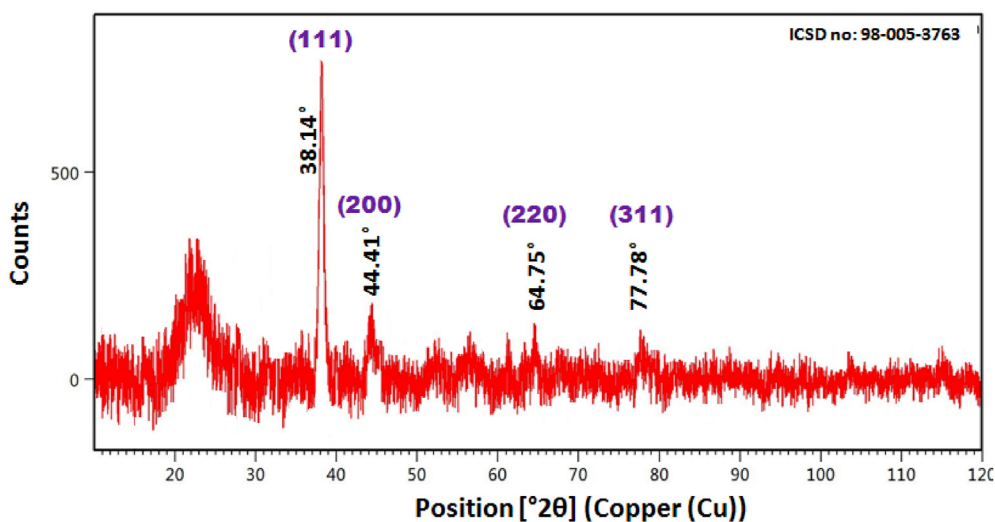


Figure 7. XRD spectrum of bee pollen synthesized AuNPs.

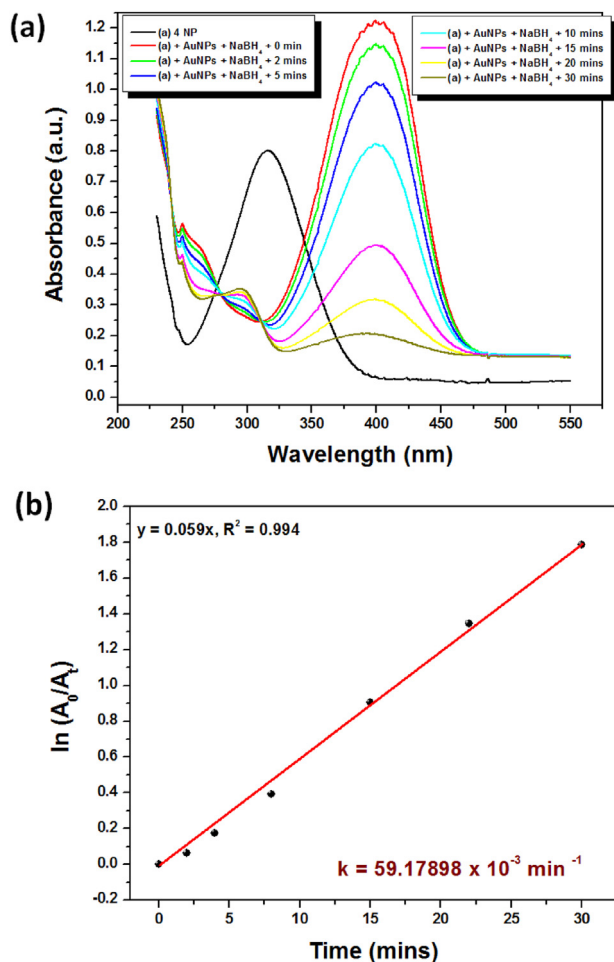


Figure 8. (a) UV-Vis spectra and (b) $\ln(A_0/A_t)$ versus time graph for reduction of 4-NP in the presence of NaBH_4 and AuNPs at 23–25 °C.

3.5. Catalytic application

Urbanization causes municipal and industrial effluence to enter the aquatic system and impacts our environment and health. To date, many techniques have been used to treat urban effluence, but each has some advantages and disadvantages. Interestingly, the remediation of toxic chemicals using biosynthesized AuNPs from plant materials offers an inexpensive and environmentally sound approach to addressing this global issue [35]. Many studies report the reduction of 4-NP in the presence of a metallic nanocatalyst. Figure 8 illustrates the catalytic reduction of 4-NP with pollen coated AuNPs at 22–25 °C using NaBH_4 as a reducing agent. The 4-NP shows an absorbance peak centered around 317 nm and λ_{max} were shifted from 317 nm to 400 nm due to 4-nitrophenolate ion formation after addition of NaBH_4 (Figure 8a) [13]. As a result of the gradual depletion of absorption sites with the passage of time and the yellow colour of the reaction mixture becomes colourless [10]. The maximum reduction capacity was achieved within 30 min (Figure 8a). In the control experiment (without AuNPs), it was observed that there was no major change in the absorption intensity of the 4-nitrophenolate ion ($\lambda_{\text{max}} = 400$ nm) at different time intervals, indicating that the reduction process was not possible in the absence of a catalyst (Figure not shown). As shown in Figure 8b, the linear relationship of $\ln(A_0/A_t)$ versus “t” was derived from the experiment, which means the 4-NP reduction followed the 1st order reaction kinetics. The rate constant (k) was estimated as $59.17898 \times 10^{-3} \text{ min}^{-1}$, $R^2 = 0.994$. It is proposed that, all reactants adsorbed on the catalyst surface and that the reaction takes place at active sites on the surface of catalyst. After that, the elec-

Table 1. Comparative table showing the various biosynthesized NPs, and their catalytic effectiveness in the reduction of 4-NP.

Biomaterial for NPs synthesis	Catalyst	λ_{max}	Size	Rate constant (k) of 4-NP	Ref.
<i>Zingiber officinale</i>	Silver NPs	432 nm	5.28 ± 1.29 nm	$2.9 \times 10^{-3} \text{ s}^{-1}$	37
<i>Limnophila rugosa</i> leaves	Silver NPs	-	87.5 nm	$3.1 \times 10^{-3} \text{ s}^{-1}$	38
<i>Cacumen platycladi</i>	Eggshell/Ag nanocomposites	420 nm	60 nm	1.56 min^{-1}	39
<i>Nephelium lappaceum</i> peel	AuNPs	563 nm	70–115 nm	$19.089 \times 10^{-2} \text{ min}^{-1}$	10
<i>Calothrix</i> algae	AuNPs	550 nm	30–120 nm	$72.4752 \times 10^{-3} \text{ min}^{-1}$	13
<i>Mangifera indica</i> leaves	AuNPs	530 nm	10–60 nm	$5.679 \times 10^{-3} \text{ s}^{-1}$	15
<i>Citrus maxima</i>	AuNPs	535 nm	25.7 ± 10 nm	$89.77 \times 10^{-3} \text{ min}^{-1}$	31
<i>Limnophila rugosa</i> leaves	AuNPs	-	122.8 nm	$2.8 \times 10^{-3} \text{ s}^{-1}$	38
<i>Rosa canina</i>	AuNPs	535 nm	26 nm	$5.08 \times 10^{-2} \text{ min}^{-1}$	40
Honeybee pollen	AuNPs	530 nm	7–42 nm	$59.17898 \times 10^{-3} \text{ min}^{-1}$	current study

tron is transferred from the BH_4^- ion (donor) to the 4-NP/4-nitrophenolate (acceptor) through AuNPs (electron relay process) and the aqueous medium supplies the necessary quantity of H^+ ions for a total reduction of 4-NP to 4-AP [36, 37, 38]. Based on catalytic reduction data for 4-NP through various biomaterial-derived NPs, the current study was compared and presented in Table 1. With this outcome, we believe that the AuNPs we have synthesized could be used for environmental remediation and catalysis applications.

4. Conclusion

In this paper, we reported a simple and cost-effective technique for the biosynthesis of AuNPs using honeybee pollen as a good reducer and stabilizer. The optical properties were studied with UV-visible spectroscopy and showed λ_{max} at 530 nm. TEM pictures showed the formation of non-aggregated, spherical, and triangular AuNPs with sizes ranging from 7 to 42 nm. FTIR confirms the presence of biomolecules like proteins polyphenol, polysaccharide, and fatty acid on the surface of AuNPs and promotes stabilization. XRD pattern demonstrated the fcc geometry and crystalline properties of AuNPs. The synthesized AuNPs serve as an efficient catalyst for the reduction from 4-NP to 4-AP with NaBH_4 and about $k = 59.17898 \times 10^{-3} \text{ min}^{-1}$. This study provides guidance to enhance the catalytic activity of pollen-based AuNPs through green synthesis and wastewater treatment.

Declarations

Author contribution statement

Brajesh Kumar: Conceived and designed the experiments; Performed the experiments; Analyzed and interpreted the data; Contributed reagents, materials analysis tools or data; Wrote the paper.

Kumari Smita: Conceived and designed the experiments; Performed the experiments; Analyzed and interpreted the data; Contributed reagents, materials analysis tools or data.

Yolanda Angulo: Performed the experiments; Analyzed and interpreted the data; Contributed reagents, materials, analysis tools or data.

Alexis Debut: Conceived and designed the experiments; Analyzed and interpreted the data; Contributed reagents, materials, analysis tools or data.

Luis Cumbal: Conceived and designed the experiments; Contributed reagents, materials, analysis tools or data.

Funding statement

Dr Brajesh Kumar was supported by Secretaría de Educación Superior, Ciencia, Tecnología e Innovación (SENESCYT) [Prometeo Project 2013–2016], Universidad de las Fuerzas Armadas ESPE [Prometeo Project 2013–2016].

Data availability statement

The authors do not have permission to share data.

Declaration of interest's statement

The authors declare no conflict of interest.

Additional information

No additional information is available for this paper.

References

- P.G. Jamkhande, N.W. Ghule, A.H. Bamer, M.G. Kalaskar, Metal nanoparticles synthesis: an overview on methods of preparation, advantages and disadvantages, and applications, *J. Drug Deliv. Sci. Technol.* 53 (2019), 101174.
- S. Ahmed, M. Ahmad, B.L. Swami, S. Ikram, A review on plants extract mediated synthesis of silver nanoparticles for antimicrobial applications: a green expertise, *J. Adv. Res.* 7 (2016) 17–28.
- M. Singh, R. Kalaivani, S. Manikandan, N. Sangeetha, A.K. Kumaraguru, Facile green synthesis of variable metallic gold nanoparticle using *Padina gymnospora*, a brown marine macroalgae, *Appl. Nanosci.* 3 (2013) 145–151.
- B. Kumar, Green synthesis of gold, silver, and iron nanoparticles for the degradation of organic pollutants in wastewater, *J. Compos. Sci.* 5 (2021) 219.
- V. Ahluwalia, S. Elumalai, V. Kumar, S. Kumar, R.S. Sangwan, Nano silver particle synthesis using *Swertia paniculata* herbal extract and its antimicrobial activity, *Microb. Pathog.* 114 (2018) 402–408.
- B. Kumar, K. Smita, E. Sánchez, A. Debut, L. Cumbal, Phytosynthesis, characterization and catalytic activity of Sacha inchi leaf-assisted gold nanoparticles, *Chem. Pap.* 76 (2022) 2855–2864.
- R. Mythili, T. Selvakumar, P. Srinivasan, A. Sengottaiyan, J. Sabastinraj, F. Ameen, A. Al-Sabri, S. Kamala-Kannan, M. Govarthanan, H. Kim, Biogenic synthesis, characterization and antibacterial activity of gold nanoparticles synthesized from vegetable waste, *J. Mol. Liq.* 262 (2018) 318–321.
- R. Mata, A. Bhaskaran, S.R. Sadras, Green-synthesized gold nanoparticles from *Plumeria alba* flower extract to augment catalytic degradation of organic dyes and inhibit bacterial growth, *Particuology* 24 (2016) 78–86.
- B. Kumar, K. Smita, A. Debut, L. Cumbal, Andean capuli fruit derived anisotropic gold nanoparticles with antioxidant and photocatalytic activity, *BioNanoScience* 11 (2021) 962–969.
- B. Kumar, K. Smita, P. Borovskikh, A. Shegolkov, A. Debut, L. Cumbal, Spectroscopic and morphological characterization of *Nephelium lappaceum* peel extract synthesized gold nanoflowers and its catalytic activity, *Inorg. Chem. Commun.* 133 (2021), 108868.
- A. Chahardoli, N. Karimia, A. Fattahi, I. Salimikia, Biological applications of phytosynthesized gold nanoparticles using leaf extract of *Dracopetalum kotschyi*, *J. Biomed. Mater. Res.* 107 (3) (2019) 621–630.
- N. Chakraborty, A. Banerjee, S. Lahiri, A. Panda, A.N. Ghosh, R. Pal, Biorecovery of gold using cyanobacteria and an eukaryotic alga with special reference to nanogold formation—a novel phenomenon, *J. Appl. Phycol.* 21 (2009) 145–152.
- B. Kumar, K. Smita, E. Sánchez, S. Guerra, L. Cumbal, Ecofriendly ultrasound-assisted rapid synthesis of gold nanoparticles using *Calothrix* algae, *Adv. Nat. Sci. Nanosci. Nanotechnol.* 7 (2016), 025013.
- M. Chokkalingam, E.J. Rupa, Y. Huo, R. Mathiyalagan, G. Anandapadmanaban, J.C. Ahn, J.K. Park, J. Lu, D.C. Yang, Photocatalytic degradation of industrial dyes using Ag and Au nanoparticles synthesized from *Angelica gigas* ribbed stem extracts, *Optik* 185 (2019) 1213–1219.
- V. Nayan, S.K. Onteru, D. Singh, *Mangifera indica* flower extract mediated biogenic green gold nanoparticles: efficient nanocatalyst for reduction of 4-Nitrophenol, *Environ. Prog. Sustain. Energy* 37 (2018) 283–294.
- I.C. Oladipo, A. Lateef, M.A. Azeez, T.B. Asafa, T.A. Yekeen, S.B. Ogunsona, H.M. Irshad, S.H. Abbas, Antidiabetic properties of phytosynthesized gold nanoparticles (AuNPs) from *Datura stramonium* seed, *IOP Conf. Ser. Mater. Sci. Eng.* 805 (2020), 012035.
- I.C. Oladipo, A. Lateef, M.A. Azeez, T.B. Asafa, T.A. Yekeen, S.B. Ogunsona, M. Irshad, A.S. Hakeem, Antifungal, anticoagulant, thrombolytic and antioxidant activities of gold nanoparticles phytosynthesized from *Blighia sapida* husk extract, *Nano: Science and Technology of Nanomaterials* 2 (2021) 1–12.
- A.E. Adebayo, A.M. Oke, A. Lateef, et al., Biosynthesis of silver, gold and silver-gold alloy nanoparticles using *Persea americana* fruit peel aqueous extract for their biomedical properties, *Nanotech. Environ. Eng.* 4 (2019) 13.
- I.C. Oladipo, A. Lateef, J.A. Elegbede, M.A. Azeez, T.B. Asafa, T.A. Yekeen, A. Akinboro, E.B. Gueguim-Kana, L.S. Beukes, T.O. Oluyide, O.R. Atanda, *Enterococcus* species for the one-pot biofabrication of gold nanoparticles: characterization and nanobiotechnological applications, *J. Photochem. Photobiol. B Biol.* 173 (2017) 250–257.
- J.A. Elegbede, A. Lateef, M.A. Azeez, et al., Biofabrication of gold nanoparticles using xylanases through valorization of corn cob by *Aspergillus niger* and *Trichoderma longibrachiatum*: antimicrobial, antioxidant, anticoagulant and thrombolytic activities, *Waste Biomass Valorization* 11 (3) (2020) 781–791.
- D. Philip, Honey mediated green synthesis of gold nanoparticles, *Spectrochim. Acta Mol. Biomol. Spectrosc.* 73 (4) (2009) 650–653.
- M. Khatami, F. Mosazade, M. Raeisi, M. Ghasemi, Z. Fazli, K. Arefkia, R.S. Varma, F. Borhani, S. Khatami, Simplification of gold nanoparticle synthesis with low cytotoxicity using a greener approach: opening up new possibilities, *RSC Adv.* 11 (2021) 3288.
- H. Banu, N. Renuka, S. Faheem, et al., Gold and silver nanoparticles biomimetically synthesized using date palm pollen extract induce apoptosis and regulate p53 and bcl-2 expression in human breast adenocarcinoma cells, *Biol. Trace Elem. Res.* 186 (2018) 122–134.
- M. Thakur, V. Nanda, Composition and functionality of bee pollen: a review, *Trends Food Sci. Technol.* 98 (2020) 82–106.
- K. Yang, D. Wu, X. Ye, D. Liu, J. Chen, Characterization of chemical composition of bee pollen in China, *J. Agric. Food Chem.* 61 (3) (2013) 708–718.
- A. Lateef, S.A. Ojo, J.A. Elegbede, The emerging roles of arthropods and their metabolites in the green synthesis of metallic nanoparticles, *Nanotechnol. Rev.* 5 (6) (2016) 601–622.
- N.K.R. Bogireddy, V. Agarwal, *Persea americana* seed extract mediated gold nanoparticles for mercury (II)/iron(III) sensing, 4-nitrophenol reduction, and organic dye degradation, *RSC Adv.* 9 (2019) 39834–39842.
- B. Kumar, K. Smita, S. Galeas, V.H. Guerrero, A. Debut, L. Cumbal, One-Pot biosynthesis of maghemite ($\gamma\text{-Fe}_2\text{O}_3$) nanoparticles in aqueous extract of *Ficus carica* fruit and their application for antioxidant and 4-nitrophenol reduction, *Waste Biomass Valorization* 12 (2021) 3575–3587.
- L. Maldonado, K. Marcinkevicius, R. Borelli, G. Gennari, V. Salomón, M.I. Isla, N. Vera, V. Borelli, Differentiation of *Argentine propolis* from different species of bees and geographical origins by UV spectroscopy and chemometric analysis, *J. Saudi Society Agri. Sci.* 19 (2020) 185–191.
- B. Kumar, K. Smita, L. Cumbal, J. Camacho, E. Hernandez-Gallegos, Maria de Guadalupe Chavez-Lopez, M. Grijalva, K. Andrade, One pot phytosynthesis of gold nanoparticles using *Genipa americana* fruit extract and its biological applications, *Mater. Sci. Eng. C* 62 (2016) 725–731.
- J. Yu, D. Xu, H.N. Guan, C. Wang, L.K. Huang, D.F. Chi, Facile one-step green synthesis of gold nanoparticles using *Citrus maxima* aqueous extracts and its catalytic activity, *Mater. Lett.* 166 (2016) 110–112.
- M. Węglińska, R. Szostak, A. Kita, A. Nems, S. Mazurek, Determination of nutritional parameters of bee pollen by Raman and infrared spectroscopy, *Talanta* 212 (2020), 120790.
- S. Zeghoud, A. Rebiai, H. Hemmami, B.B. Seghir, N. Elbouhdiri, S. Ghareba, D. Gheraout, N. Abbas, ATR–FTIR spectroscopy, HPLC chromatography, and multivariate analysis for controlling bee pollen quality in some Algerian regions, *ACS Omega* 6 (2021) 4878–4887.
- E. Turunc, O. Kahraman, R. Binzet, Green synthesis of silver nanoparticles using pollen extract: characterization, assessment of their electrochemical and antioxidant activities, *Anal. Biochem.* 621 (2021), 114123.
- S.A. Akintelu, B. Yao, A.S. Folorunso, Bioremediation and pharmacological applications of gold nanoparticles synthesized from plant materials, *Heliyon* 7 (2021), e06591.
- A. Bhattacharjee, M. Ahmaruzzaman, A green approach for the synthesis of SnO_2 nanoparticles and its application in the reduction of p-nitrophenol, *Mater. Lett.* 157 (2015) 260–264.
- G. Dinda, D. Halder, A. Mitra, N. Pal, D.K. Chattoraj, Phytosynthesis of silver nanoparticles using *Zingiber officinale* extract: evaluation of their catalytic and antibacterial activities, *J. Dispersion Sci. Technol.* 41 (14) (2020) 2128–2135.
- V.T. Le, N.N.Q. Ngu, T.P. Chau, T.D. Nguyen, V.T. Nguyen, T.L.H. Nguyen, X.T. Cao, V.-D. Doan, Silver and gold nanoparticles from *Linnophila rugosa* leaves: biosynthesis, characterization, and catalytic activity in reduction of nitrophenols, *J. Nanomater.* (2021) 11. Article ID 5571663.
- X. Huang, L. Changa, Y. Lua, Z. Li, Z. Kang, X. Zhang, M. Liu, D.-P. Yang, Plant-mediated synthesis of dual-functional Eggshell/Ag nanocomposites towards catalysis and antibacterial applications, *Mater. Sci. Eng. C* 113 (2020), 111015.
- P.E. Cardoso-Avila, R. Patakfalvi, C. Rodriguez-Pedroza, X. Aparicio-Fernandez, S. Loza-Cornejo, V. Villa-Cruz, E. Martinez-Canob, One-pot green synthesis of gold and silver nanoparticles using *Rosa canina* L. extract, *RSC Adv.* 11 (2021) 14624–14631.